Carbon Attrition During the Fluidized Combustion of a Coal

The generation of carbon fines by attrition during the fluidized combustion of a bituminous coal has been studied by means of a 140mm ID fluidized-bed combustor under variable excess air factor, bed temperature, fluidizing velocity and size of bed sand and coal. Results indicate that rates of attrited fines are roughly proportional to excess of gas velocity above the minimum for fluidization and bed carbon exposed surface. Attrition rate constant is affected by size of sand and, to a less extent, and particularly with finer coal, by bed temperature.

U. ARENA, M. D'AMORE and L. MASSIMILLA

Istituto di Chimica Industriale e Impianti Chimici
Università Istituto di Ricerche sulla Combustione
Napoli, Italy

SCOPE

The loss of carbon fines is one of the major drawbacks to an efficient and environmentally acceptable utilization of coal by means of fluidized combustion. In some circumstances, the rates of elutriated unburned carbon are as high as 10–15% of the fixed carbon charged into the combustor (Archer et al., 1971; Poersch and Zabeschek, 1980). Unburnt carbon fines are entrained in the exit gas stream, from which they must be separated by means of cyclones, and either recycled to the bed or burned in ancillary equipment under appropriate conditions.

Previous studies (Donsì et al., 1979; Cammarota et al., 1981), have shown that attrition or, possibly, fragmentation and attrition in combination, might be relevant to carbon elutriation and loss of efficiency in the fluidized combustion of a South African bituminous coal. Rather high rates of elutriated carbon fines were in fact found in operating a 140 mm ID fluidized-bed combustor even with coal of 6–9 mm size, i.e., with a feed without fines and so coarse that the contribution to carbon elutriation by residues from combustion of particles originally charged into the bed should have been negligible. Relationships between rates of elutriated carbon formed by attrition, bed carbon loading and exposed surface, and excess of gas velocity above the minimum for fluidization were suggested as a result of these studies.

Experiments have been furthered, using the same coal, with the scope of: 1) testing previous relationships throughout the entire range of bed temperatures of interest in fluidized combustion and for various excess air factors, fluidizing velocities and coal feed sizes; 2) characterizing particle-size distributions of attrited carbon under various experimented conditions; 3) investigating the influence of size of bed inert material on carbon attrition; and 4) determining attrition behavior of the coal tested under conditions of fluidized combustion.

CONCLUSIONS AND SIGNIFICANCE

Analysis of rates and particle-size distributions of elutriated carbon lead to a simple model of carbon fines generation during the fluidized combustion of the coal tested. It considers fragmentation of coal feed particles in relatively coarse subparticles as a preliminary stage, with combustion and significant attrition of fragmented subparticles following in parallel to each other. Attrition is enhanced by combustion, as suggested by results of comparative tests carried out fluidizing coal in hot beds of sand under inert conditions.

Roughly, elutriation rates of attrited carbon are directly proportional to the product of the excess of gas velocity above the minimum for fluidization and overall carbon surface exposed to attrition inside the bed. Data scattering is mostly related to residual effects of bed temperature on attrition rate constant in addition to the effects that changes in this variable produce on bed carbon loading and average particle size and, as a consequence, on carbon exposed surface. Results suggest that bed temperature somewhat directly affects the mechanism of generation of carbon fines, particularly when feeding relatively fine coal.

Increase of attrition rate constant by a factor of about six is found when increasing bed sand size within the range tested. A problem open by this work is how much this increase is to be related to the enhanced rate of generation of carbon fines, in respect to possible reduction of rate of in-bed postcombustion of such fines when using coarser bed material.

Research on particle attrition in fluidized beds has been considerably forwarded by the development of fluidized coal combustion systems. Attention, however, has been mainly devoted to the attrition behavior of coal ashes and of limestones and dolomites (Merrick and Highley, 1974; Vaux, 1978; Franceschi et al., 1980; Chen et al., 1980) in relation to problems of atmospheric pollution control and better utilization of sorbents. Studies on the mechanism of carbon particle combustion in fluidized beds have generally been carried out on the assumption that the fraction of feed carbon leaving the combustor as attrited fines is negligible (Avedesian and Davidson, 1973; Chakraborty and Howard, 1980). But this assumption is not necessarily valid under all experimental conditions.

D'Amore et al. (1980) suggested that, for coal burning according to the shrinking particle model, carbon combustion and attrition can be considered as parallel phenomena. Therefore, the instantaneous shrinkage rate and carbon combustion efficiency of a bed carbon particle, assumed of spherical shape with a diameter d, are respectively expressed by the relationships:

$$-\frac{dd}{dt} = \left(-\frac{dd}{dt}\right)_c + \left(-\frac{dd}{dt}\right)_a \qquad (1)$$

0001-1541-83-6425-0040-$2.00.

and

$$\eta_c = \frac{\left(\frac{dd}{dt}\right)_c}{\left(\frac{dd}{dt}\right)_c + \left(\frac{dd}{dt}\right)_a} \tag{2}$$

where $(dd/dt)_c$ is the rate of shrinkage due to combustion and $(dd/dt)_a$ that due to attrition. Accordingly, any change in the design or operative variables of the combustor affecting the rate of combustion of the bed carbon particles results in a change of combustion efficiency, unless it is not compensated by an equal change in the rate of attrition. Namely, a decrease in the combustion efficiency due to loss of attrited carbon has been found by operating at lower bed temperature, with inherently less reactive fuels, with coarser fuel feed sizes, at lower excess air or with an uneven air distribution at the bottom of the bed, (D'Amore et al., 1980; Cammarota et al., 1981). All these changes produce in fact a reduction of $(-dd/dt)_c$. On the basis of the two phase theory of fluidization, assuming perfect mixing of gas in the particulate phase and plug flow of bubble phase (Campbell and Davidson, 1975), with fast devolatilization of coal and burning of volatiles, it is:

$$\left(-\frac{dd}{dt}\right)_c = c_p \frac{1}{\frac{d\rho_c}{2M_c \mathrm{Sh} D_g} + \frac{\rho_c}{2M_c k_s}} = \left\{c_i - \frac{F_{O_{2,v}} + (F_c - E_c)/M_c}{A[U - (U - U_o)e^{-x}]}\right\} \frac{1}{\frac{d\rho_c}{2M_c \mathrm{Sh} D_g} + \frac{\rho_c}{2M_c k_s}} \tag{3}$$

where c_i and c_p are the oxygen concentrations in the inlet air and in the particulate phase; $F_{O_{2,v}}$ and $(F_c - E_c)/M_c$, the molar flow rates of oxygen consumed inside the bed for burning volatiles and fixed carbon; A, the combustor cross section; Sh, the carbon particle Sherwood number; D_g, the oxygen diffusivity; ρ_c, the bed carbon density; k_s the carbon surface reaction rate constant at the particle effective temperature; U and U_o, the fluidization and the minimum fluidization velocity; X, the number of transfer units for gas exchange between the bubble and the particulate phases.

Literature models of fluidized bed coal combustors generally neglect the contribution of attrited carbon fines to the rates of elutriated carbon (Beér et al., 1977; Chen and Saxena, 1978; Park et al., 1979; Wells et al., 1980). But this first approximation approach can result in an unacceptable overestimation of carbon combustion efficiency under conditions of practical interest. Beér et al. (1980) evaluated the rates of elutriated carbon due to attrition by using Eq. 1 (based on particle radius instead of diameter) to account for the overall rate of particle shrinkage due to combustion and attrition in the particle population balance equation of Kunii and Levenspiel (1968). The attrition component was:

$$\left(-\frac{dd}{dt}\right)_a = k_a(U - U_o) \tag{4}$$

as derived on the assumption of a rate of carbon loss due to attrition proportional to carbon particle external surface and excess of gas velocity U above the minimum velocity for fluidization U_o (D'Amore et al., 1980). Calculation results indicated that for feed particle size in the range of 0.5–3 mm the contribution of attrited carbon fines to the overall carbon loss is rather large, even when using a conservative value for the attrition rate constant k_a.

Note that Eq. 4 is consistent with the relationship used by Donsì et al. (1977), to correlate rates of attrited carbon E_c''', carbon loading W_c, and surface-based average bed carbon particle size $\bar{d}$:

$$E_c''' = k\frac{(U - U_o)W_c}{\bar{d}} \tag{5}$$

where:

$$\bar{d} = \frac{1}{\sum_{d}^{d_{co,max}} \frac{X_d}{d}} \tag{6}$$

with $d_{co,max}$ the maximum size of coal feed particles and X_d the mass fraction of bed carbon of size d. Equation 5 suggests in fact that the overall rate of attrited carbon is proportional to $(U - U_o)$ and $W_c/\bar{d}$ which, for given carbon particle density, represents the overall carbon surface exposed in the bed to attrition. It can be shown (Donsì et al., 1980) that $k_a = k/3$.

EXPERIMENTAL

The combustor used, 140 mm ID, is schematically shown in Figure 1. Air was fed at the bottom through a pipe-type distributor. Fuel was supplied by means of a screw feeder. Bed height, indirectly read at a manometer measuring pressure drop across the bed, was kept at the desired level without overflow. With the coal tested most ashes were in fact elutriated as fines. Additions of inert bed material (sand) were necessary to compensate for bed solids sampling. Bed temperature was maintained at the desired level by means of a 9 mm OD cooling coil, 84 cm long, located close to the wall. Most of the free board was left unlagged in order to favour gas cooling and prevent postcombustion of carbon fines. Typical temperature profiles along the bed and free board are reported in Figure 2.

The combustor could be operated in various arrangements as regards the height of the free board (2 or 4 m), the nozzle overall cross-sectional area of the air distributor (1.3 or 5.8 cm^2), the entrance cross-sectional area of the cyclone first state (2.6 or 10.6 cm^2). Change from one arrangement to the other was made when necessary to extend operative ranges of fluidizing velocity under conditions suitable to measuring rates of carbon

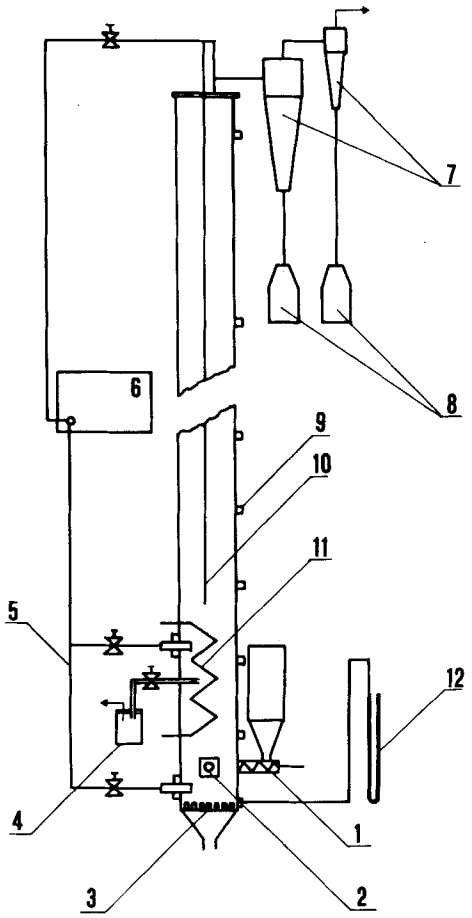

Figure 1. Experimental apparatus: 1) screw feeder; 2) statrt-up burner; 3) pipe distributor; 4) bed solids sampling bottle; 5) gas sampling line; 6) gas analyzers; 7) cyclone; 8) fines collecting bottle; 9) thermocouple; 10) gas sampling probe; 11) cooling coil; 12) manometer.

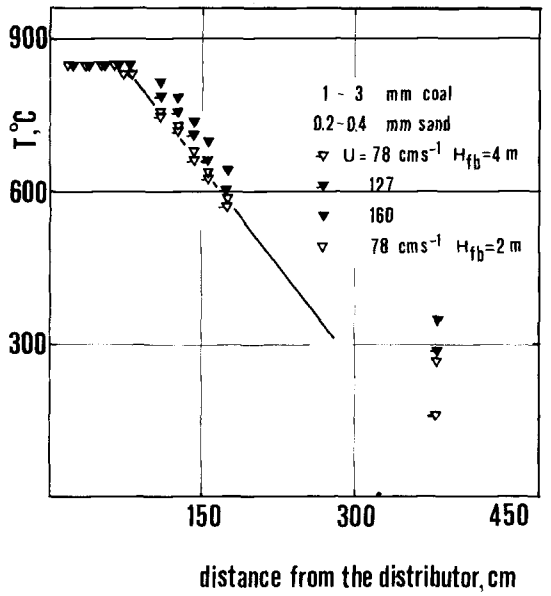

Figure 2. Axial temperature profiles of the combustor.

attrition inside the bed. In particular, the free board height was kept high enough to meet TDH requirements (Zenz and Weil, 1958) under all the fluidizing velocities. Attrition related to air injection and solids separation system was minimized by limiting outlet velocity at distributor orifices and inlet velocity in the first stage of cyclone. A check on the effectiveness of these provisions was made by comparing results for various arrangements (D'Amore et al., 1980, Cammarota et al., 1981). The completeness of collection of elutriated carbon was occasionally tested with a third high efficiency cyclone in series to the two-stage cyclone ordinarily used.

Properties of the coal used are reported in Table 1. Results of tests aiming at identifying the attrition behavior of this coal in hot fluidized bed under inert conditions are reported in Table 2. A bench-scale combustor 40 mm ID and 1.1 m high, described in detail elsewhere (Cammarota et al., 1980), was used for these tests. Experiments were carried out batchwise, dropping coal particles in the bed of sand, kept at 850°C by means of external heating and fluidized by nitrogen. Rates of attrited carbon per unit bed carbon loading $(E_c''')_i/W_c$ are given within various time intervals from the injection of the coal into the bed. The rates of carbon fines within the first minute are relatively higher than those collected later. They might have been somewhat affected by the production of elutriable fines during coal fragmentation, which occurs at that stage of the test because of devolatilization. Note, however, that the amounts of such elutriable fines are small in respect to the amount of coal undergoing fragmentation. On the basis of present data and results of the Chirone (1980) study on fragmentation of the same coal during combustion, the fraction of fragmented carbon subparticles entrained in the carryover is estimated to be, at most, $1 \cdot 10^{-3}$ of the coal injected into the bed.

Table 3 reports the ranges of variables tested, including coal feed sizes. Within the limits of experimental feasibility, appropriate combinations

TABLE 1. PROPERTIES OF COAL TESTED

South African Coal		
Calorific Value Net, kcal·kg^{-1}		6,280
Proximate Analysis, % on Dry Basis:	Fixed Carbon	60
	Volatile Matter	25
	Ash	15
Ultimate Analysis, % on Dry Basis:	Carbon	74.3
	Hydrogen	4.7
	Oxygen	5.5
	Sulfur	0.5
	Ash	15.0
Free Swelling Index (ASTM D720)		1-2
Hardgrove Grindability Index (ASTM D 409)		51
Ash Fusion Temperature Reducing Atmosphere		
Carbolite Furnace (Pyramids)	Deformation	1,400°C
	Hemispherical	1,400°C
	Flow	1,400°C

TABLE 2. RESULTS OF ATTRITION TESTS OF COAL UNDER INERT CONDITIONS

40 mm ID combustor; quiescent bed height, 10 cm; T = 850°C; sand, 0.2–0.4 mm; fluidizing gas, nitrogen.

d_{co}, mm	U, cm·s^{-1}	$(E_c''')_i/W_c \cdot 10^3$, min^{-1} Collection Times 0–1 min	1–3 min	3–33 min
0.4–1	78	1.4	0.58	0.17
1–3	78	0.25	0.14	0.04
1–3	160	0.82	0.22	0.14

of the values of these variables were chosen in performing the 59 runs whose results are reported in the following. Time intervals of 1–2 hours were required between two consecutive runs to reach, for selected values of the operative variables, the steady state regime of the combustor as regards outlet gas composition, bed carbon loading and particle size distribution, and carbon elutriation rates. The achievement of the steady state for each run was controlled by recording oxygen concentration in outlet gas and comparing results of analyses of at least two samples of solids from the bed and two from the cyclone, taken at a distance of time of about a hour one from the other.

For each run, measurements of bed carbon loading and particle-size distribution were made by sampling solids at the midpoint of the expanded bed. The validity of this technique was tested by a parallel investigation on coal particles distributions in fluidized beds of the various sand sizes. This was carried out at room temperature under conditions as regards the size of coal, the size of sand and the fluidizing velocity more critical from the standpoint of coal segregation. Coal concentrations measured along the bed were determined by bed sectioning (Nienow et al., 1978), and compared with the average expected for perfect mixing on the basis of weights of sand and coal charged to the combustor. Coal concentration proratios reported in Figure 3 show the reliability of the bed midpoint sampling technique for coal feed size as those used in the present work, and coarser. Carbon loadings were obtained by multiplying carbon mass fraction of bed solids sampling by the weight of bed solids. Bed carbon size distributions were determined by sieving bed solids samples and measuring the carbon content C of each mass fraction X_{d_b} of size d, as shown for a typical run in Table 4. The product $X_{d_b} \cdot C$ gave the amount of carbon in each size fraction, free of ash and bed sand. Normalization of the values of $X_{d_b} \cdot C$ gave X_d, the mass fraction of bed carbon of size d. This procedure, assumes the absence of particles made partly of carbon, partly of ash.

Elutriated carbon rates were determined as the products of the rates of collection of solids at the cyclone and carbon mass fraction of the collected material. Elutriated carbon-size distributions were determined on the basis of sieve and carbon content analyses as also shown in Table 4. Again, the absence of elutriated fine particles made partly of carbon and partly of ash was assumed, although micrographs taken at high magnification ratio with an optical microscope showed that this could not be so. Size classification of solids below 45 μm was made by means of Coulter Counter technique. Carbon analyses, however, were not available for these finer fractions. It was assumed that the average carbon content measured for the material below 45 μm applied to each fraction in the range 45–0 μm. Note that carbon content in the various fractions of elutriated carbon decreases

TABLE 3. EXPERIMENTAL CONDITIONS

Operative Variables of the Combustor	
Quiescent Bed Height, cm	33
Free Board Height, cm	200, 400
Bed Temperature, °C	650, 700, 750, 850, 950
Fluidizing Velocity, cm·s^{-1}	78, 127, 160
Excess Air Factor	0.9–1.4
Silica Sand Sizes, mm	0.2–0.4, 0.4–0.6, 0.6–0.85, 0.85–1, 1–1.4

Size Distributions of the Coal (Measured Downstream the Screw Feeder)

0.4–1 mm Nominal Size		1–3 mm Nominal Size	
d, μm	$X_{d_{co}}$, %	d, μm	$X_{d_{co}}$, %
1,000–850	21.42	3,000–2,360	27.36
850–600	41.76	2,360–2,000	16.54
600–425	34.49	2,000–1,700	18.53
425–300	2.24	1,700–1,400	15.38
300–212	0.09	1,400–1,000	21.04
212	/	1,000–800	1.15
		800	/
$\bar{d}_{co}$ = 0.65 mm		$\bar{d}_{co}$ = 1.77 mm	

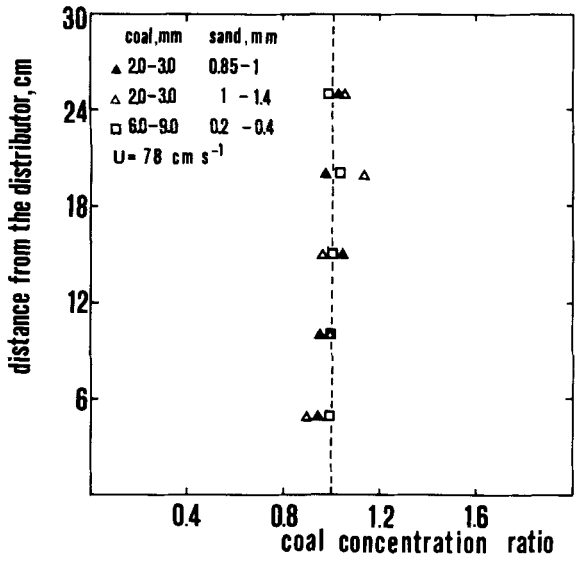

Figure 3. Ratios of measured to expected coal concentrations at various bed heights.

regularly as fraction size decreases. The exceptionally low value of C (and high value of $X_{\delta_{cy}}$) for 212–125 μm reflects the contribution of the elutriation of the finer particles of the sand in determining the overall amount of material collected at the cyclone.

TABLE 4. SIZE DISTRIBUTION OF BED CARBON AND OF ELUTRIATED CARBON COLLECTED AT CYCLONE FOR A TYPICAL RUN

Experimental Conditions of the Run

coal, 1–3 mm; sand, 0.2–0.4 mm; H_{fb} = 4 m; T = 850°C; e = 1.02; U = 160 cm·s^{-1}; U' = 88 cm·s^{-1}; d^* = 250 μm; F_{co} = 53.4 g·min^{-1}; F_c = 32.03 g·min^{-1}; E_c = 2.55 g·min^{-1}; W_c = 254 g; $\bar{d}'_{co}$ = 1.64 mm; $\bar{d}$ = 1.46 mm

Size Distribution of Bed Carbon (°)

d, μm	X_{d_b}, %	C, % g/g	X_{d_b}·C	X_d, %
3000–2360	21.68	54.22	11.75	25.97
2360–2000	11.34	58.86	6.67	14.75
2000–1700	13.62	58.29	7.94	17.55
1700–1400	10.42	51.86	5.40	11.94
1400–1000	17.08	45.73	7.81	17.26
1000–250	25.86	21.91	5.67	12.53

Size Distribution of Elutriated Carbon

δ, μm	$X_{\delta_{cy}}$, %	C, % g/g	$X_{\delta_{cy}}$·C	X_δ, %	
>250	1.00	47.35	0.47	1.69	Coarser than 45 μm,
250–212	1.25	47.20	0.59	2.12	based on sieve
212–125	16.44	24.30	4.00	14.39	analysis
125–90	4.14	44.08	1.82	6.55	
90–75	3.62	44.67	1.62	5.83	
75–63	2.57	43.83	1.13	4.07	
63–53	3.57	36.93	1.32	4.75	
53–45	3.22	38.94	1.25	4.50	
45.0–40.3	1.16		0.28	1.01	finer than 45 μm,
40.3–32.0	2.31		0.56	2.02	based on Coulter
32.0–25.4	4.04		0.98	3.53	Counter analysis
25.4–20.2	6.10		1.48	5.33	
20.2–16.0	7.06		1.71	6.15	
16.0–12.7	6.61		1.61	5.79	
12.7–10.1	6.03		1.47	5.29	
10.1– 8.0	5.39	average	1.31	4.71	
8.0– 6.3	5.26		1.28	4.61	
6.3– 5.0	4.56	C = 24.29	1.11	3.99	
5.0– 4.0	3.98		0.97	3.49	
4.0– 3.2	3.79		0.92	3.31	
3.2– 2.5	3.21		0.78	2.81	
2.5– 2.0	2.70		0.66	2.37	
2.0– 1.6	1.09		0.26	0.94	
1.6– 1.3	0.51		0.12	0.43	
1.3– 1.0	0.39		0.09	0.32	

( ) = sieve analysis made on bed solids sample properly treated to preseparate sand (Donsì et al., 1978).

DISCUSSION

Estimation of Rates of Carbon Attrition from Data of Carbon Fines Elutriation

A result found in the experiments carried out in the present work, as well as in that of Ross (1980), is that the number of particles collected at the cyclone is much larger than that of coal particles charged into the bed. Combustion alone cannot explain this finding, because it simply produces a reduction in the size of the particles. Fragmentation and attrition, instead increase the number of particles. This analysis is based on the assumption that carbon fines generation during the fluidized combustion of the coal tested depends on fragmentatin of coal feed particles, and combustion and attrition of fragmented subparticles. Fragmentation and attrition are related to different phenomena. Fragmentation is due to devolatilization of coal soon after it is charged into the bed, and results in the break-up of feed particles into pieces, most of which of relatively coarse size (Chirone, 1980). Attrition is due to the rubbing of carbon particles against bed material and the wall of the combustor while they are burning inside the bed, and produces fines which detach from the surface of the mother particles. Accordingly, the rate E_c of elutriated carbon collected at the cyclone is made of the contribution of the rates of carbon elutriation due to: 1) elutriable fines originally charged with feed coal and formed during fragmentation, E'_c; 2) fines resulting as elutriable residues from combustion and attrition of subparticles formed by feed coal fragmentation, E''_c and 3) fines formed by attrition of these subparticles while burning in the bed, E'''_c. It is

$$E_c = E'_c + E''_c + E'''_c \tag{7}$$

Available data are used to evaluate the relative importance of E'_c, E''_c and E'''_c for the coal and experimental conditions tested, and, in particular, to estimate E'''_c. Postcombustion shall be disregarded in this analysis, assuming that rates of generation of attrited carbon are represented by values of E'''_c as obtained from data of carbon collection at the cyclone. Actually, whereas postcombustion of attrited material in the free board could be minimized by proper experimental arrangement, that inside the bed could not be affected at all, as it takes place in the same environment as attrition. E'''_c, therefore, is not exactly the rate of generation of attrited carbon fines. It really is the algebraic sum of the rates of carbon attrition and in-bed postcombustion. Moreover, accumulation in the bed of carbon fines adhering to bed carbon particles has been neglected.

As an example, evaluation of E'_c E''_c and E'''_c shall be based on the result of the run of Table 4, carried out at 850°C, with 1–3 mm coal feed and fluidizing velocity of 160 cm·s^{-1}. As regards E'_c, for a gas velocity at the cyclone outlet U' of 88 cm·s^{-1}, d^*, the size of carbon particle with terminal velocity equal U', is about 250 μm. Being this value lower than the finer fraction of the coal feed (Table 3), the contribution to E'_c of fines originally contained in the coal charge is inexistent. The contribution to E'_c of fines formed during fragmentation is also negligible, as pointed out before in commenting on carbon fines collection in the first minute of coal attrition tests under inert conditions (Table 2). Accordingly, E'_c can be neglected and Eq. 7 reduces to

$$E_c = E''_c + E'''_c \tag{8}$$

As defined above, E''_c is the elutriation rate of carbon subparticles as they shrink from the size d'_{co} to the size of $d^* = 250$ μm, at which they are entrained in the carryover. Using size distributions of fragmented subparticles measured by Chirone (1980), E''_c is calculated as follows:

$$E''_c = F_c \sum_{d^*}^{d'_{co,max}} \left(\frac{d^*}{d'_{co}}\right)^3 X_{d'_{co}} \tag{9}$$

where F_c is the fixed carbon feed rate and $X_{d'_{co}}$, the mass fraction of particles of size d'_{co}. For experimental conditions in consider-

TABLE 5. COMPARISON BETWEEN MEASURED RATES OF ELUTRIATED CARBON AND ESTIMATED RATES OF ATTRIATED CARBON FOR TYPICAL RUNS

T = 850°C; sand: 0.2–0.4 mm

d_{co}	U	F_{co}	W_c	E_c	E_c'''	$E_c/W_c \cdot 10^3$	$E_c'''/W_c \cdot 10^3$
mm	cm·s^{-1}	g·min^{-1}	g	g·min^{-1}	g·min^{-1}	min^{-1}	min^{-1}
0.4-1	78	24.5	26.3	1.00	0.62	38.0	23.6
1-3	78	25.9	178	1.07	1.04	6.0	5.8
1-3	160	53.4	254	2.55	2.39	10.0	9.4

ation, this gives $E_c'' = 5 \cdot 10^{-3}$. $F_c = 0.16$ g·min^{-1}. With such value of E_c'', Eq. 8 gives $E_c''' = E_c - E_c'' = 2.39$ g·min^{-1}, i.e., a rate of elutriated carbon related to attrition rather close to E_c. Particle-size distribution of carbon collected at the cyclone shows that E_c''' is a very large fraction of E_c in this case. Only 1.69% of elutriated carbon E_c has in fact a size coarser than $d^* = 250$ μm, and 2.12% a size between 250 and 212 μm. Similar analysis applies to runs carried out with 0.4–1 mm coal. In this case, however, the estimated contribution of residues to overall carbon elutriation is relatively higher, as shown in Table 5. Equation 9, in fact, results in larger E_c'' as the d^*/d'_{co} ratios increase.

The abundance of material of size much lower than d^* in the solids at cyclone confirms the important role of attrition in carbon fines generation. Curves of cumulative size distributions of attrited carbon particles relative to three experimental conditions a, b and c have been selected for presentation in Figure 4. Curve b has been evaluated on the basis of data in the fourth column of Table 4, cutting the distribution to the size $d^* = 250$ μm, and normalizing. A similar procedure has been used for the other curves a and c. The selection has been made with the criterion of comparing size distribution for experiments with the same sand (0.2–0.4 mm) and different fluidizing velocity (78 and 160 cm·s^{-1}), and with the same velocity (160 cm·s^{-1}) and different sands (0.2–0.4 mm and 1–1.4 mm). The displacement of curve b in respect to a is explained to some extent by the fact that increasing the fluidizing velocity, the size d^* of elutriable carbon particle increases. Coarser material is collected at the cyclone under condition c, which suggests that sand size might have some effect on the size of carbon fines generated by attrition and/or on their in-bed postcombustion.

The comparison between rates of attrited carbon collected in combustion experiments and in tests with nitrogen fluidized beds is not straightforward because the latter were carried out batchwise. A rough estimation of the effect of combustion on attrition can be made comparing the values E_c'''/W_c for combustion runs (Table 5) and the values $(E_c''')_i W_c$ found at various times in tests under

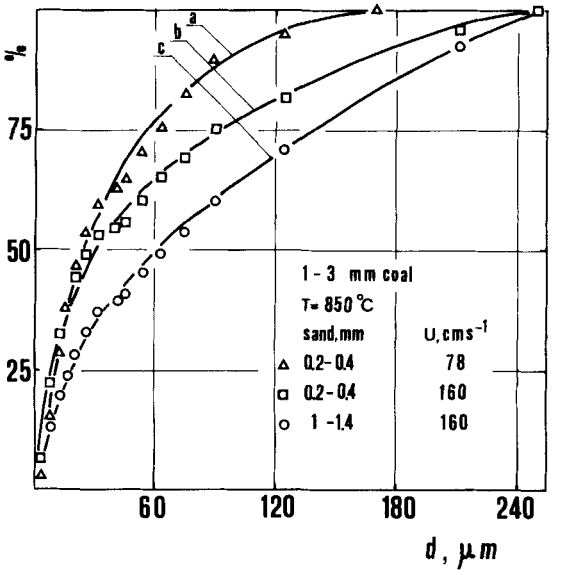

Figure 4. Cumulative particle size distributions of carbon fines collected at cyclone.

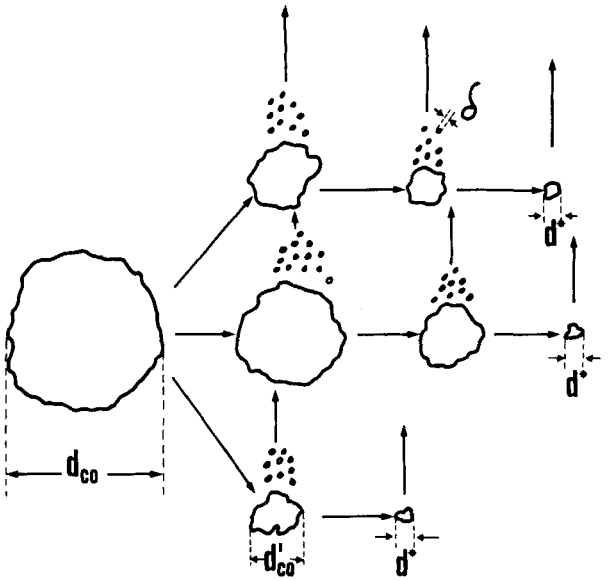

Figure 5. Model representation of carbon fines generation in the fluidized combustion of the coal tested.

inert conditions (Table 2). Values of E_c'''/W_c are one or two orders of magnitude larger than $(E_c''')_i/W_c$, depending on whether this ratio is referred to the first or the later thirty minutes of collection after coal injection into the bed. This suggests that detachment of carbon fines from a hot fluidized carbon particle is more active when the particle is burning than when it is inside an inert environment, in spite of the fact that the intensity of its rubbing against bed solids and the wall of the combustor is the same in the two cases.

According to above analysis and results, a model of carbon fines generation in the fluidized combustion of the coal tested is suggested in Figure 5. It considers the fragmentation of the coal feed particle in coarse subparticles as a preliminary stage, with combustion and substantial attrition of subparticles following in parallel to each other. As now available, the model is not expected to be of general application. It might offer, however, a reference framework when extending measurements of attrition during fluidized combustion to other coals. Changing coal may require changing the model structure or merely accounting for the different rates at which various steps take place and sizes distribution of solids they produce.

Dependence of Rates of Attrited Carbon on Variables of Combustor

Operative variables of the combustor, namely: bed temperature, fluidizing velocity, excess air factor and size of coal and bed sand, affect rates of attrited carbon as well as bed carbon loading and particle size distribution, i.e., the bed carbon exposed surface. These dependences will be discussed in parallel, with a view to expressing rates of carbon attrition as a function of bed carbon exposed surface and excess of gas velocity above the minimum for fluidization.

Bed carbon size distribution is negligibly affected by changes in bed sand size and excess air factor e, and only limitedly by changes in fluidizing velocity U and bed temperature T, as shown in Figure 6. For comparison, coal feed size distributions are reported in this illustration. Note that the spread between feed coal and bed carbon size distribution increases with the coal feed size range used. Similar finding resulted from the experiments with coal up to 6–9 mm size reported previously (Cammarota et al., 1981).

The influence of bed temperature on the rates of attrited carbon E_c''' is shown in Figure 7 for 0.4–1 mm and 1–3 mm coal, and for various factors of excess air. It appears that the increase of both T and e results in a decrease of E_c'''. Also, for given T and e, E_c''' for

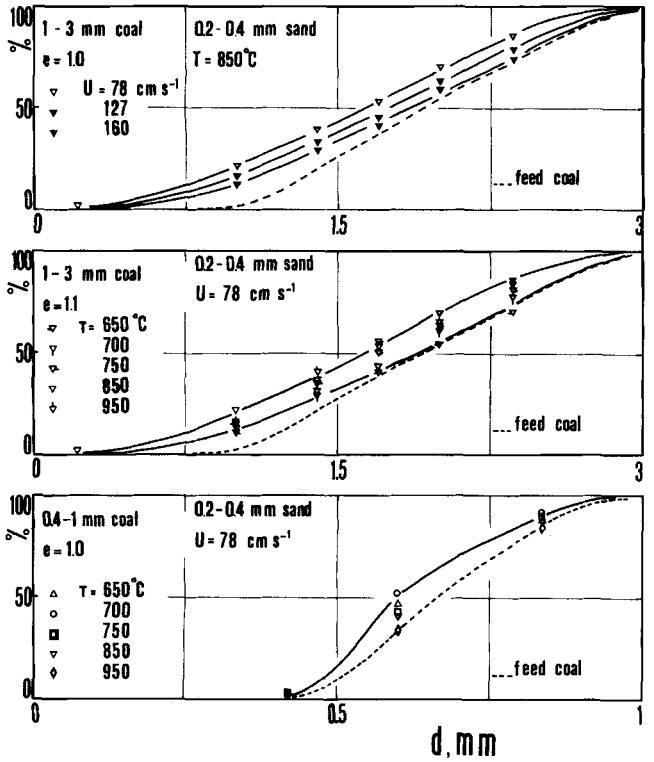

Figure 6. Cumulative bed carbon particle size distributions.

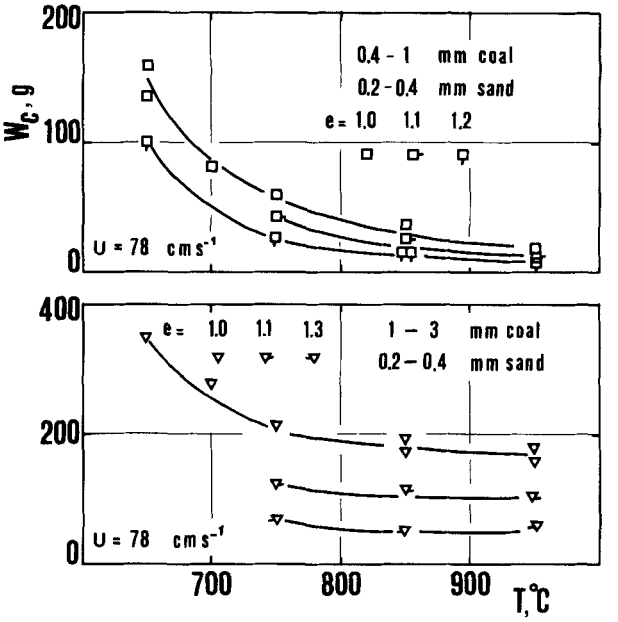

Figure 8. Bed carbon loadings as a function of bed temperature.

0.4–1 mm is lower than for 1–3 mm coal. Bed carbon loadings W_c in Figure 8 show similar trends in response to changes in T, e and coal feed size. As regards W_c, such trends are related to the effect of these variables on the shrinkage rate of carbon particle, which in turn affects carbon loading. In fact, under steady state conditions, increasing or decreasing $(-dd/dt)_c$ respectively tends to decrease or increase the number of particles required in the bed to ensure the combustion of a given coal feed rate and, as a consequence, W_c. In particular, Eq. 3 suggests that $(-dd/dt)_c$ is raised by an increase of e and T, and a decrease of coal feed size. These changes respectively result in the increase of the particulate phase oxygen concentration c_p, in the decrease of the kinetic resistance term $(\rho_c/2M_c k_s)$ and in the decrease of the diffusional resistance term $(d\rho_c/2M_c \mathrm{Sh} D_g)$. It is consistent with the theory that substantial changes in W_c with T are particularly found when operating with finer coal (Figure 8). With 1–3 mm coal the diffusional component of the overall resistance to particle combustion prevails, and, being it slightly affected by temperature, changes of W_c as a function of T are limited. Note also that with this coarser coal the overall resistance to carbon particle combustion is larger and, as a consequence, W_c is also larger.

The similarity in the trends of E_c vs. T and W_c vs. t in Figures 7 and 8, respectively, reflects the simple relationships $E_c = k'''W_c$ found by Donsì et al. (1979). These are presented in Figure 9, where, as in the following illustrations, the slopes k''' of the straight lines were calculated by least squares. For 1–3 mm and 0.4–1 mm coal k''' varies with T between $7.3 \cdot 10^{-3}$ and $4.3 \cdot 10^{-3}$ min^{-1}, and $42 \cdot 10^{-3}$ and $16 \cdot 10^{-3}$ min^{-1}, respectively. Using bedcarbon particle-size distributions reported in Figure 6, size averages $\bar{d}$ were obtained according to Eq. 6 and values of $W_c/\bar{d}$, which are pro-

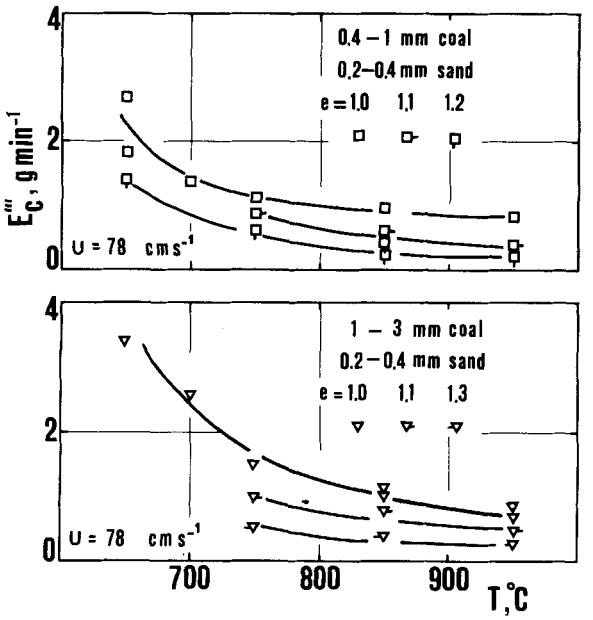

Figure 7. Elutriation rates of attrited carbon as a function of bed temperature.

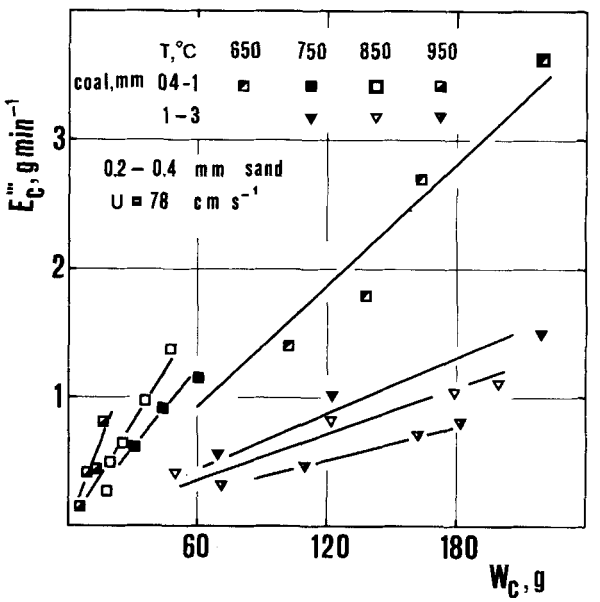

Figure 9. Elutriation rates of attrited carbon as a function of bed carbon loading for various coal feed sizes and bed temperatures.

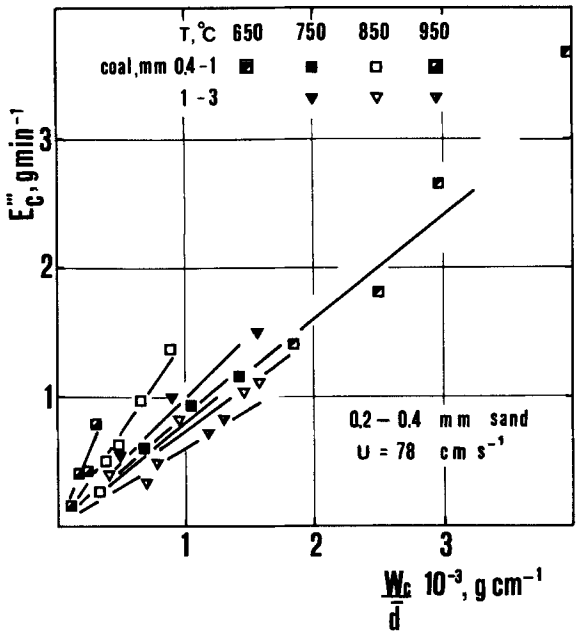

Figure 10. Elutriation rates of attrited carbon as a function of exposed bed carbon surface.

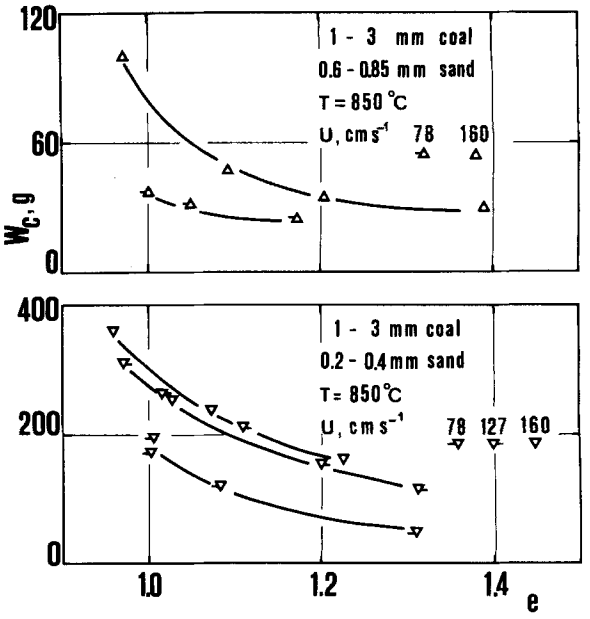

Figure 12. Bed carbon loadings as a function of excess air factor.

portional to the exposed surface of carbon in the bed, calculated. Figure 10 shows that values of E_c''' from the series of experiments with 0.4–1 mm and 1–3 mm coal fall much closer to each other when plotting $E''' = k''W_c/\bar{d}$. Changing to $W_c/\bar{d}$, however, does not reduce the spread of the values of k'' relative to various bed temperatures in respect to that observed for k''' when plotting E_c''' as a function of W_c. It is so because the influence exerted by bed temperatures on $\bar{d}$ is small, as expected from particle size distributions in Figure 6.

Figure 9 (and 10) show that, within a given feed coal size, k''' (and k'') vary with T, with a trend which is different for the two series of experiments. For 1–3 mm coal, k''' (and k'') decreases with T, whereas for 0.4–1 mm coal it increases. Changes of k''' (and k'') for 1–3 mm coal might be related to different degrees of postcombustion of carbon fines at variable temperatures, but this explanation does not apply to the case of 0.4–1 mm coal feed. Apparently with finer feed coal, bed temperature tends to foward the rate of generation of carbon fines more than that of their postcombustion. It is difficult, however, to establish whether such influence is displayed towards attrition or fragmentation. As the size of feed coal decreases below 1 mm, sizes of attrited fines tend to be comparable to sizes of fragments and, as shown by Chirone (1980), fragmentation results become unreliable.

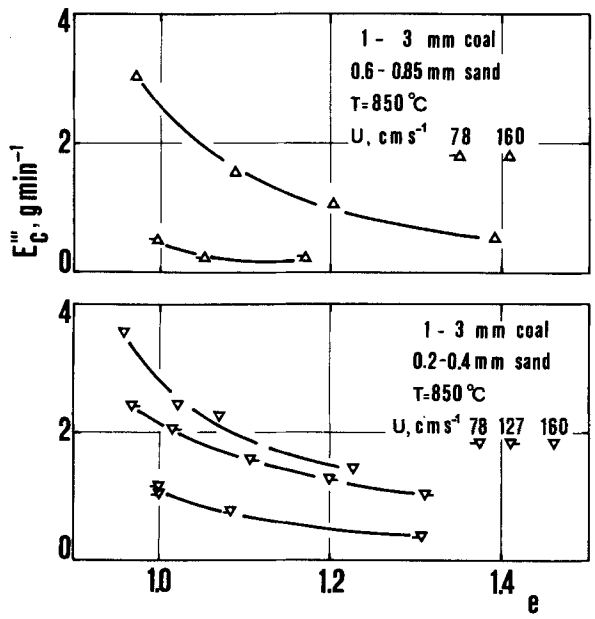

Figure 11. Elutriation rates of attrited carbon as a function of excess air factor.

Rates of elutriated attrited carbon E_c''' for feed coal 1–3 mm are reported as a function of e and variable fluidizing velocity U in Figure 11 for 0.2–0.4 mm and 0.6–0.85 mm sand. The decrease of e and the increase of U produce an increase of E_c'''. Also, both these changes result in an increase of W_c, as shown in Figure 12. There are two results deserving consideration in this latter illustration, namely: 1) the considerably smaller value of W_c when using, other experimental conditions remaining the same, the coarser sand and 2) the small increase of W_c when changing U from 127 to 160 cm·s^{-1}. The first, which confirms early observation by Donsì et al. (1978), is explained in terms of an increased $(-dd/dt)_c$, since, as shown by Eq. 3, with coarser sand, the oxygen concentration in the particulate phase c_p is enhanced by both the reduction of $(U - U_o)$ and the increase of X. The second, cannot be explained immediately. Probably increasing U, $(-dd/dt)_c$ increases because $F_{O_2,e}$ decreases, due to the fact that a larger portion of volatiles burns in the freeboard leaving more oxygen available for carbon combustion in the particulate phase. In spite of this uncertainty, all the data in Figures 11 and 12 follow the simple relationship $E_c''' = k'''W_c$, as shown in Figure 13.

The slopes k''' tend to change with the size of the sand and, for the same sand, with U. Figure 14 shows that the values of E_c''' for a given sand collect on the same straight line if, following Donsì et al. (1979), rates of elutriated, attrited carbon are plotted as a function of $(U - U_o)W_c$, being $E_c''' = k'(U - U_o)W_c$. There are, however, different slopes k' for sands of different size. Altogether, these data and those from experiments with 0.4–0.6 mm, 0.85–1 mm and 1–1.4 mm sand, also plotted in the same illustration, suggest that there is a gradual increase in the rates of elutriated carbon as, for given $(U - U_o)W_c$, sand size increases.

Change in sand size may affect the rates of elutriated carbon by modifying both the rates of generation by attrition of carbon fines and the rates of their in-bed postcombustion. The relative relevance of these effects, however, cannot be easily established. Concerning postcombustion, it may be argued that two opposite trends may be expected by the increase of sand size. On one side, higher rates of postcombustion of carbon fines, due to the increased oxygen

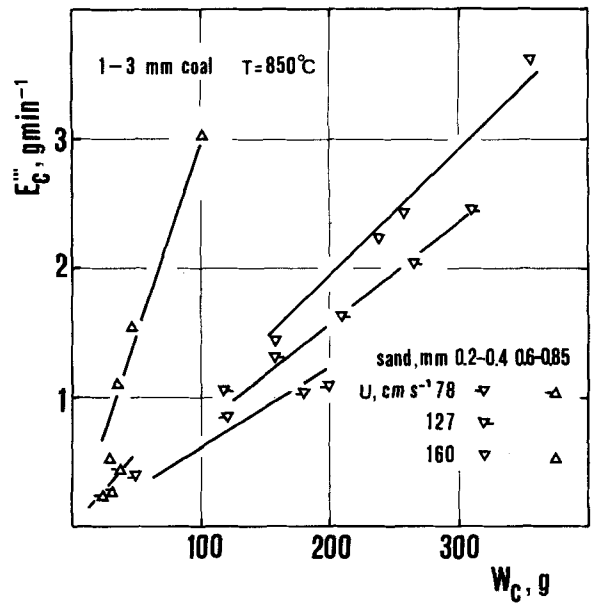

Figure 13. Elutriation rates of attrited carbon as a function of bed carbon loading for various sand sizes and fluidizing velocities.

concentration in the particulate phase. On the other, lower rates, because of the presumably lower residence time of fines in such phase, due to the larger interparticle spacings and higher interstitial gas velocity. This latter trend is in the observed direction, but, quantitatively, not such to exclude that, under the experimental conditions tested, increasing sand size had also the parallel effect of raising considerably the number of carbon particles generated by attrition per unit time. Curves of particle-size distributions in Figure 4 show in fact that attrited carbon fines in the case of sand 0.2–0.4 mm are finer than those relative to sand 1–1.4 mm, but not so much as to justify a degree of postcombustion reducing of about one sixth the value of k'. Further experimental work should test various combinations of feed coal and bed solids particles sizes, as well as bed solids of various hardness.

The correlation of E'''_c as a function of $(U - U_o)W_c/\bar{d}$, according

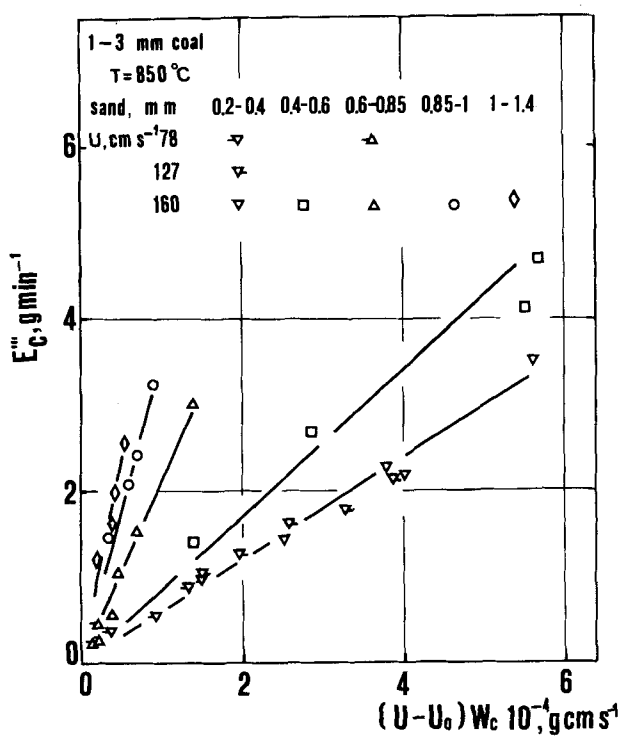

Figure 14. E'''_c vs $(U - U_o)W_c$ correlation.

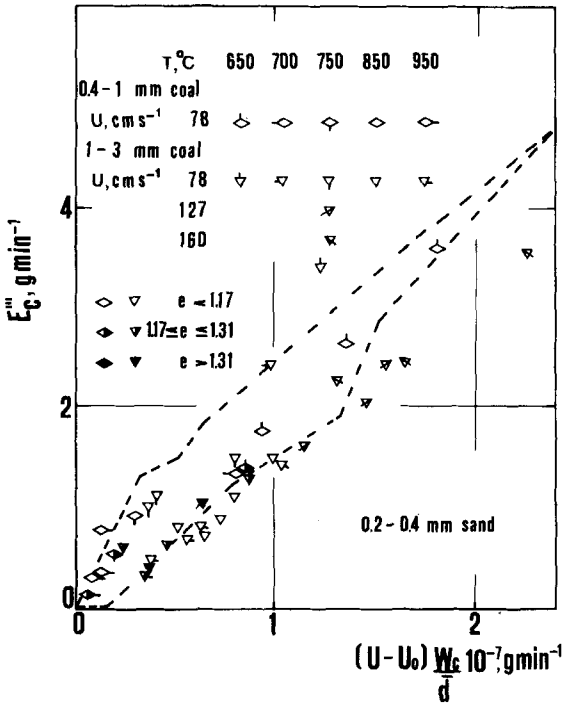

Figure 15. E'''_c vs $(U - U_o)W_c/\bar{d}$ correlation.

to Eq. 5 for the 37 runs with 0.2–0.4 mm sand is reported in Figure 15. Data scattering in respect to the straight line $E''' = k(U - U_o)W_c/\bar{d}$ reflects the influence of bed temperature already mentioned in discussing Figure 10. Data points of the previous sets of experiments (Donsì et al., 1979; Cammarota et al., 1981) carried out with 0.2–0.4 mm sand, bed temperature of 850°C, fluidizing velocity between 50 and 130 cm·s^{-1}, and coal feed between 0.4–1 mm and 6–9 mm, fell in the dotted area. The value of k based on all the 121 data available is $1.86 \cdot 10^{-7}$, with a standard deviation of $0.33 \cdot 10^{-7}$. The value of k previously given was $2.1 \cdot 10^{-7}$. The degree of uncertainty associated with this attrition rate constant is fairly acceptable when considering the width of the ranges of experimental variables. It is likely that such value of k can be extrapolated to coal size larger than 9 mm but not lower than 0.4 mm. With finer coal the model of Figure 5 itself becomes unreliable because of ambiguity between fragmentation and attrition.

Values of the attrition rate constant k have been also calculated from data of experiments with other sands. Figure 16 shows that

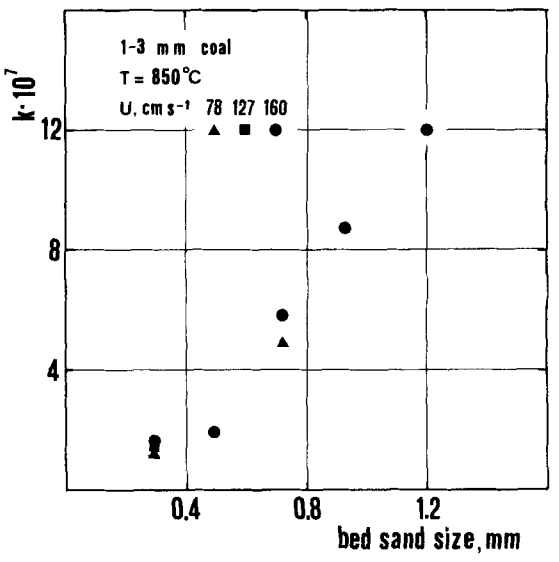

Figure 16. Attrition rate constant k as a function of bed sand size.

k decreases rather regularly for sands from 1–1.4 mm to 0.4–0.6 mm, then it tends to level off. One might argue that k for 0.2–0.4 mm sand roughly gives the asymptote of the values of the attrition rate constant as bed sand becomes very small, although data now available do not allow one to support this conclusion.

It should also be borne in mind that attrition rate constants given as a result of this work were obtained from experiments carried out under conditions as much as possible controlled as regards post-combustion in the free board. This aspect deserves special consideration when comparing between each other attrition rate constants measured with different fluidized combustors, or when using them in model calculations of combustors for which active postcombustions in the free board are expected.

ACKNOWLEDGMENTS

This work has been carried out under the sponsorship of the Progetto Finalizzato Energetica, financed by the G.N.R., Roma. Authors are indebted to G. Donsì for useful discussion and to A. Cammarota, Ing. G. Capasso and Ing. B. Farina who helped in performing the experimental work. Coulter Counter analyses of material collected at the cyclone have been made at ENEL- CRTN in Pisa. One of the Authors (U.A.) is grateful to Ansaldo S.p.A., Genova, for providing a scholarship.

NOTATION

A = bed cross section
c_i = oxygen concentration in the inlet air
c_p = oxygen concentration in the particulate phase
C = percentage carbon content
$d, \bar{d}$ = bed carbon particle and surface based average particle size
d^* = size of the shrunken particle with terminal velocity equal to gas velocity at the free board outlet temperature
$d_{co}, \bar{d}_{co}$ = feed coal particle and surface based average particle size
$d'_{co}, \bar{d}'_{co}$ = fragmented coal subparticle and surface based average subparticle size
D_g = oxygen diffusivity
e = excess air factor
E_c, E'_c, E''_c, E'''_c = carbon elutriation rates
$(E'''_c)_i$ = carbon elutriation rate in tests under inert conditions
F_c = fixed carbon feed rate
F_{co} = coal feed rate
$F_{O_{2,v}}$ = oxygen molar flow rate required for combustion of volatiles in the particulate phase
H_{fb} = free board height
k, k', k'', k''', k_a = carbon attrition rate constants
k_s = carbon surface reaction rate constant
M_c = carbon atomic weight
Sh = carbon particle Sherwood number
T = bed temperature
U = fluidizing gas superficial velocity at bed temperature
U' = gas superficial velocity at the free board outlet temperature
U_o = minimum fluidizing gas superficial velocity at bed temperature
W_c = bed carbon loading
X = number of transfer units
X_d = mass fraction of bed carbon particles of size d
X_{d_b} = mass fraction of bed particles (carbon, sand and ash) of size d
$X_{d_{co}}$ = mass fraction of size d_{co} in feed coal
$X_{d'_{co}}$ = mass fraction of size d'_{co} *in coal after fragmentation*
$X\delta$ = mass fraction of carbon particles collected at cyclone of size δ
$X_{\delta_{cy}}$ = mass fraction of particles collected at cyclone (carbon, sand and ash) of size δ
δ = size of carbon fines
μ = carbon combustion efficiency
ρ_c = bed carbon density

LITERATURE CITED

Archer, D. H., D. L. Keairns, and J. R. Hamm, "Evaluation of the Fluidized Bed Combustion Process. II Technical Evaluation," *Nat. Tech. Inform. Serv. PB Rep.*, Westinghouse Research Lab., Pittsburgh (1971).

Avedesian, M. M., and J. F. Davidson, "Combustion of Carbon Particles in a Fluidized Bed," *Trans. Instn. Chem. Engrs.*, **51**, 121 (1973).

Beér, J. M., R. E. Baron, G. Borghi, J. L. Hodges, and A. F. Sarofim, "A Model of Coal Combustion in Fluidized Bed Combustors," 5th Int. Conf. on Fluidized Combustion, DOE, Washington, DC (Dec., 1977).

Beér, J. M., L. Massimilla, and A. F. Sarofim, "Fluidized Coal Combustion: the Effect of Coal Type on Carbon Load and Carbon Elutriation," Int. Conf. on Fluidized Combustion: Systems and Applications, Institute of Energy Symp. Ser., No. 4, London (Nov., 1980).

Cammarota A., M. D'Amore, G. Donsì, and L. Massimilla, "Fluid Bed Combustion of a Sulcis Lignite," *La Termotecnica*, **XXXIV**, No. 2, 61 (1980).

Cammarota, A., M. D'Amore, G. Donsì, and L. Massimilla, "Attrition of Carbon Particles in Fluidized Combustion," Fluidized Combustion Conference, Energy Research Institute, Cape Town, S.A. (Jan., 1981).

Campbell, E. K., and J. F. Davidson, "The Combustion of Coal in Fluidized Beds," Institute of Fuel Symp. Ser., No. 1, *Fluidized Combustion*, London (Sept., 1975).

Chakraborty, R. K., and J. R. Howard, "An Experimental Study of Mechanism of Combustion of Carbon in Shallow Fluidized Beds," *Fluidization*, eds. J. R. Grace and J. M. Matsen, Plenum Press, New York (1980).

Chen, T. P., and S. C. Saxena, "A Mechanistic Model Applicable to Coal Combustion in Fluidized Beds," *AIChE Symp. Ser.*, No. 176, **74**, 149 (1978).

Chen, T. P., C. I. Sishtla, D. V. Punwani, and H. Arastoopour, "A Model for Attrition in Fluidized Beds," *Fluidization*, eds. J. R. Grace and J. M. Matsen, Plenum Press, New York (1980).

Chirone, R., "Coal Fragmentation During Fluidized Bed Combustion," Thesis in Chemical Engineering, University of Naples (1980).

D'Amore, M., G. Donsì, and L. Massimilla, "Bed Carbon Loading and Particle Size Distribution in Fluidized Combustion of Fuels of Various Reactivity," 6th Int. Conf. on Fluidized Bed Combustion, DOE, Atlanta, GA (April, 1980).

Donsì, G., L. Massimilla,, G. Russo, and P. Stecconi, "Carbon Load and Gas Composition in a Fluidized Bed Combustor," Proceedings of the 17th Symp. (Int.) on Combustion, Leeds, England (August, 1978).

Donsì, G., L. Massimilla, and M. Miccio, "Carbon Fines Production and Elutriation from the Bed of a Fluidized Coal Combustor," IRFF Chemical Panel, Pisa, April 1979, *Combustion and Flame*, **41**, 57 (1981).

Donsì, G., L. Massimilla, and M. Miccio, "The Elutriation of Solid Carbon from a Fluidized Bed Combustor," *La Rivista dei Combustibili*, **XXXIV**, 336 (1980).

Franceschi, J. F., An Kolar, G. Miller, V. Zakkay, C. Ho, W. Skelley, and S. Hakim, "Natural Sorbent Attrition Studies Related to Fluidized Bed Coal Combustion," 6th Int. Conf. on Fluidized Bed Combustion, DOE, Atlanta, GA (April, 1980).

Kunii, D., and O. Levenspiel, "Fluidisation Engineering," J. W. Wiley, New York (1969).

Merrick, D., and J. Highley, "Particle Size Reduction and Elutriation in a Fluidized Bed Process," *AIChE Symp. Ser.*, No. 137, **70**, 366 (1974).

Nienow, A. N., P. N. Rowe, and T. Chiba, "Mixing and Segregation of a Small Proportion of Large Particles in Gas Fluidized Beds of Considerably Smaller Ones," *AIChE Symp. Ser.*, No. 176, **74**, 45 (1978).

Park, D., O. Levenspiel and T. J. Fitzgerald, "A Model for Large Scale Atmospheric fluidized Bed Combustor," paper 26c, 72nd Annual AIChE Meeting, San Francisco (Nov., 1979).

Poersch, W., and G. Zabeschek, "Fluidised Combustion of Fuels with Different Ash Contents," Int. Conf. on Fluidized Combustion: Systems

and Applications, Institute of Energy Symp. Ser., No. 4, London (Nov., 1980).
Ross, I., J. F. Davidson Report at Int. Conf. Fluidized Combustion, Systems and Applications, Institute of Energy Symp. Ser., No. 4, London (Nov., 1980).
Vaux, W. G., "Attrition of Particles in the Bubbling Zone of a Fluidized Bed," Proceedings of the American Power Conference (1978).
Wells, J. W., R. P. Kirshnan, and C. E. Ball, "A Mathematical Model for Simulation of AFBC System," 6th Int. Conf. on Fluidized Bed Combustion, DOE, Atlanta, GA (April, 1980).
Zens, F. A., and N. A. Weil, "A Theoretical-Empirical Approach to the Mechanism of Particle Entrainment from Fluidized Beds," *AIChE J.*, No. 4, 4, 472 (1958).

Manuscript received June 19, 1981; revision received October 16, and accepted January 13, 1982

Feasible Specifications in Azeotropic Distillation

Feasible operating conditions are obtained for an azeotropic distillation tower using a nonlinear programming algorithm. The boil-up rate, fractional recovery of product, and bottoms purities of entrainer and by-product are adjusted to locate an overhead vapor stream that condenses into two liquid phases, but is in equilibrium with a single liquid phase on the top tray. A new objective function is introduced and minimized, subject to inequality constraints, using Powell's algorithm (1977). Results are obtained for dehydration of alcohol with benzene.

G. J. PROKOPAKIS and W. D. SEIDER

Department of Chemical Engineering
University of Pennsylvania
Philadelphia, PA 19104

SCOPE

In a classical paper, Benedict and Rubin (1945) define azeotropic distillation as "a process in which the substance added forms an azeotrope with one or more of the components and by virtue of this fact is present on most of the plates of the column in appreciable concentration." This definition correctly places emphasis on the need to select a mass separating agent that forms an azeotrope with one of the species to be separated, rather than the need to "break" an azeotrope.

Furthermore, a suitable entrainer, in the words of Benedict and Rubin, "forms non-ideal solutions with one or both of the components and thereby exaggerates the difference in volatility between them." Normally, entrainer is fed on the top tray, forming a low-boiling azeotrope with one or both of the species. Vapor with composition approaching the azeotrope is condensed and, for heterogeneous systems, the entrainer phase is decanted for reflux, as illustrated in Figure 1, for dehydration of alcohol.

In the typical configuration, one or more towers concentrate dilute alcohol to compositions approaching the alcohol-water azeotrope (shown schematically as a single processing step). In Figure 1a, nearly complete recovery of high purity alcohol is achieved in the azeotropic tower. The overhead vapor is condensed, a fraction is sent to a decanter, and the remainder is combined with the entrainer phase from the decanter and a small entrainer make-up stream as reflux to the azeotropic tower. The aqueous phase from the decanter is fed to the stripping tower, where nearly all of the water in the feed to the azeotropic tower is recovered in high purity. The overhead vapor, containing alcohol and water with some entrainer, is condensed and recycled to the decanter. Similar configurations have a common condenser with a portion of the condensate bypassing the decanter or a portion of the aqueous phase from the decanter recycled for reflux to the azeotropic tower. Such a decanter bypass stream or aqueous reflux is usually necessary to permit steady operation of the azeotropic tower with high recovery of alcohol in a high-purity bottoms product. Furthermore, for steady operation, these streams can be adjusted to respond to small changes in feed composition or product purity. The make-up stream replaces entrainer lost in parts-per-million concentration from the azeotropic and stripping towers.

In Figure 1b, the alcohol fed to the azeotropic tower is not entirely recovered. Instead alcohol and water in the bottoms of the stripping tower are recycled to the alcohol concentrators where water is recovered and alcohol is recirculated.

Azeotropic towers have been in operation for many years, but it is only recently that mathematical models have been sufficient to accurately trace the steep fronts in concentration and temperature. (See Figure 7, for example.) These fronts are extremely sensitive to small differences in the concentrations of entrainer and water in the nearly pure bottoms product and to the boil-up rate (Prokopakis and coworkers, 1981; Magnussen and coworkers, 1979). Furthermore, these variables must be carefully adjusted to prevent the models from predicting a vapor overhead stream that cannot be condensed to form two liquid phases, requiring that the overhead vapor stream from the stripping tower be condensable into two liquid phases, giving a high concentration of alcohol in the stripper bottoms, and low recovery of alcohol in the azeotropic tower.

In fact, it became so difficult to avoid operating conditions with low recovery of alcohol in the azeotropic tower, that we found it necessary to develop a strategy to avoid this problem. This has been accomplished by formulating a nonlinear programming problem with an appropriately selected objective function and inequality constraints.

0001-1541-83-6006-0049-$2.00.
G. J. Prokopakis is currently at Columbia University, New York, N.Y.